Ballistocardiography for Cardiac Output Estimation: Towards Non-Invasive Monitoring in Medical Emergencies

Sara Entenza [1], Iraia Isasi [1], Johannes Nordsteien Svensøy [2], Robert Beck [2], Lars Wik [2], Erik Alonso [1]

[1] University of the Basque Country (UPV/EHU), Bilbao, Spain
[2] Division of Prehospital Services, Oslo University Hospital, Oslo, Norway

Abstract

Currently, no automated, non-invasive, and robust method exists to monitor blood circulation and guide treatment in prehospital emergency medicine. Cardiac output (CO) monitoring could provide a solution, but CO monitors are neither feasible nor practical in the prehospital setting. Non-invasive ballistocardiography (BCG) measures cardiac contractility and reflects changes in CO. The aim of this study was to analyze the feasibility of estimating CO using morphological features extracted from BCG signals. The study database included a total of 125 segments extracted from 20 healthy subjects. Each segment contained ECG, carotid and abdominal BCG signals, and CO obtained via invasive blood pressure. BCG signals were processed using adaptive filtering and the stationary wavelet transform to isolate the circulatory component of the BCG. Then, using a nested cross-validation architecture, the most relevant features were extracted and selected from the circulatory components, and a support vector regression model was fitted to estimate CO. The resulting model achieved a mean absolute error of 0.96 L/min and a relative error of 14%. This method represents a promising first step toward an automated, non-invasive, and robust CO estimator that could be tested in prehospital emergencies.

1. Introduction

Out-of-hospital cardiac arrest (OHCA) is the abrupt cessation of effective cardiac mechanical activity outside the hospital setting, resulting in loss of pulse and consciousness. It represents a critical public health problem, with approximately 340,000 annual deaths in adults in the US and a survival rate with good neurological outcome of 9.0% [1]. Early detection of OHCA enables prompt initiation of cardiopulmonary resuscitation (CPR) and timely bystander defibrillation, which can double survival rates [2]. Likewise, optimal post-resuscitation care is essential for improving long-term outcomes in survivors [3]. Both OHCA recognition and post-resuscitation care rely on the reliable identification of the absence and presence of circulation, respectively. Conventional methods for assessing circulation in OHCA present important limitations: carotid pulse palpation is unreliable and was excluded from clinical guidelines in 2005 [4], agonal breathing can be mistaken for normal breathing [5], and ECG-based pulse identification struggles to differentiate pulseless electrical activity (PEA) from pulse-generating rhythm, since both can present quasi-normal QRS complexes.

Various methods based on the processing of biomedical signals acquired by defibrillation equipment have been proposed to detect pulse during OHCA, with ECG and thoracic impedance being the most widely used signals. Despite this, their implementation has not been carried out, as it requires substantial hardware modifications to commercial devices that manufacturers are not willing to undertake. As an alternative, cardiac output (CO), defined as the volume of blood pumped by the heart per unit of time, could provide a more accurate assessment of circulation. However, its reference measurement via pulmonary catheterization is invasive and therefore infeasible in prehospital settings.

Thus, ballistocardiography (BCG) emerges as a non-invasive, low-cost option, traditionally recorded using piezoelectric or force sensors that capture whole-body recoil forces produced by cardiac activity. Unlike this traditional whole-body approach, this study employs local piezoelectric BCG sensors placed directly over the carotid and abdominal aortic pathways, as previously validated by Svensøy et al. [6]. This configuration captures localized mechanical displacements associated with the propagation of the ejected blood volume, offering a more portable and clinically deployable alternative to whole-body BCG.

2. Materials

An observational study was conducted, designed to simulate a real OHCA scenario with 20 healthy individuals, in the cardiology department of Oslo University Hospital. Each subject was placed in a supine position on

an ambulance stretcher with: (1) LIFEPAK® 15 monitor/defibrillator (Stryker) pads in anterolateral position for ECG; (2) a FloTrac sensor connected via a radial arterial line to a HemoSphere monitor (Edwards Lifesciences) for invasive blood pressure and CO calculation via pulse waveform analysis; and (3) two piezoelectric BCG biosensors (Kopera Norway AS) over the carotid artery and abdominal aorta, connected via USB to a laptop for BCG signal recording.

The protocol comprised six phases: normoventilation (9 min), hyperventilation (1 min), hypoventilation (30 s), Trendelenburg positioning (2 min), ambulance transport (5 min), and infusion of 500 mL of Ringer's acetate (4 min). Hyperventilation and transport were excluded due to breathing and motion artifacts, respectively.

Accordingly, the study database consisted of 125 segments with a mean (standard deviation, SD) duration of 48.6 (42.3) s. Specifically, 27/19/29/50 segments with a mean (SD) duration of 41.1(27.6)/ 30.1(7.1)/ 45.7(28.0)/ 61.3(57.6) s corresponded to the normoventilation/hypoventilation/Trendelenburg/infusion phases, respectively. Each segment included ECG, carotid BCG (BCGc), abdominal BCG (BCGc), and CO signals (Figure 1).

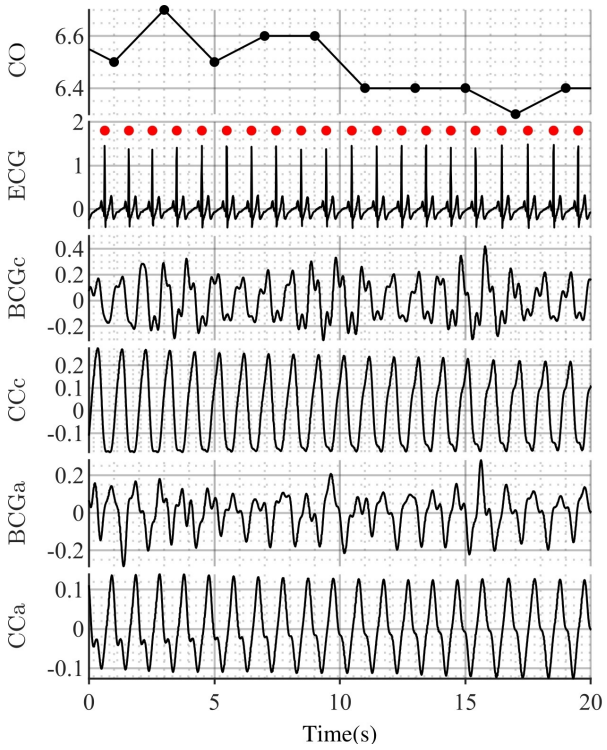

Figure 1. Example of a 20-second segment showing, from top to bottom, CO, preprocessed ECG, preprocessed BCGc, CCc, preprocessed BCGa, and CCa.

3. Methodology

CO estimation was carried out following a multi-stage process applied to 10 s signal segments with 80% overlap. First, the ECG was preprocessed using a 0.5–30 Hz band-pass filter, while the BCGc and BCGa signals were filtered with a 0.5-3 Hz band-pass filter to remove low- and high-frequency artifacts, as well as baseline fluctuations. Second, the circulatory component was extracted from the BCGc and BCGa signals through the sequential use of i) an adaptive filtering scheme, and ii) a multiresolution analysis based on the stationary wavelet transform. Third, a process of extraction and selection of the most relevant features from the circulatory components was carried out. Finally, an SVR model was fitted and optimized to perform the final CO estimation.

3.1. Extraction and multiresolution analysis of the circulatory component

Healthy subjects have a pulse, so the BCG signal, $s_{bcg}(n)$, can be expressed through the following additive model $s_{bcg}(n) = s_{rest}(n) + CC(n)$, where the sample index n relates to time through $t = \frac{n}{f_s}$, with sampling frequency $f_s = 250$ Hz. $s_{rest}(n)$ contains the baseline and artifacts mostly due to sensor movement and sensor-skin contact. Each effective cardiac contraction ejects blood into the aorta and generates fluctuations in the BCG. These fluctuations precisely constitute the circulatory component $CC(n)$. Consecutive fluctuations vary slightly in amplitude and duration, as the morphology of CC(n) is hypothesized to reflect the force and dynamics of ventricular ejection transmitted through the arterial wall, which are primary determinants of stroke volume and, consequently, of CO. Therefore, $CC(n)$ exhibits a quasi-periodic nature and can be modeled using a Fourier series with N terms whose amplitudes and frequencies vary slowly over time:

$$CC(n) = \sum_{k=1}^{N} a_k(n)\cos(k\omega_0(n)n) + b_k(n)\sin(k\omega_0(n)n)$$

where the in-phase and quadrature coefficients are represented by $a_k(n)$ and $b_k(n)$, respectively, and the fundamental frequency is given by $\omega_0(n) = 2\pi f_0(n)/f_s$. The computation of $f_0(n)$ was carried out using the following equation:

$$f_0(n) = \frac{f_s}{r_{i+1} - r_i} \quad \forall n \in (r_i, r_{i+1}]$$

where r_i represents the sample index of the R peak of the i-th QRS complex. QRS complexes were automatically detected using the Hamilton-Tompkins algorithm (represented by the red dots in the ECG shown in Figure 1). The coefficients $a_k(n)$ and $b_k(n)$ were estimated

using the recursive least squares (RLS) algorithm, with forgetting factor λ governing the trade-off between convergence speed and stability.

The circulatory component was then decomposed into 8 levels using a Coiflet-3 stationary wavelet transform (SWT), yielding detail coefficients $d_1 - d_8$ and approximation coefficients $a_1 - a_8$. The reconstructed signal, $s_{cc}(n)$, retained only subbands $d_6 - d_8$ (0.5–3.9 Hz), containing relevant hemodynamic information; the remaining coefficients were set to zero.

3.2. Feature extraction

A total of 103 features were extracted, grouped into two sets. The first includes 66 features derived from the reconstructed circulatory components s^a_{cc} (abdominal) and s^c_{cc} (carotid), capturing morphological properties of each beat (duration, amplitude, area, length) and statistical distribution (standard deviation, skewness, kurtosis). The second set comprises 36 features from the ensemble average of the detail coefficients $d^a_6 - d^a_8$ (abdominal) and $d^c_6 - d^c_8$ (carotid), representing beat-to-beat average patterns while removing transient variability.

3.3. Model architecture and evaluation

A nested cross-validation (CV) architecture was used to train the model and evaluate its performance. The inner loop consisted of a 4-fold CV scheme for feature selection using a filter approach and for optimizing the hyperparameters of the regression model, while a 5-fold CV scheme was applied in the outer loop to evaluate model performance. In both the inner and outer loops, quasi-stratified random partitions were used at the patient level. Given the limited number of subjects, all segments belonging to the same patient were assigned to the same fold in both the inner and outer loops, preventing data leakage across training and test partitions.

Model performance was evaluated in terms of mean absolute error (MAE), computed by comparing the CO predictions estimated by the model with the reference values obtained via the HemoSphere system. The nested CV procedure was repeated 50 times using different random partitions to estimate the statistical distribution of the MAE.

Feature selection was carried out using the RReliefF algorithm, which estimates predictor relevance from the 14 nearest neighbors (Euclidean distance) of each instance, weighting predictors whose variation aligns with changes in CO and penalizing those that fluctuate independently of it.

An SVR with a Gaussian kernel was selected, and its hyperparameters C and γ were optimized. The cost parameter C regulates the SVR's bias-variance trade-off, and γ defines the kernel's adaptability to the data. The hyperparameters C and γ were tuned in the inner loop through a grid search over the ranges $0.6 \leq C \leq 1.02$ and $10 \leq \gamma \leq 10.4$ to minimize the MAE of the SVR model.

4. Results and discussion

Figure 2 shows the heatmap of the average MAE obtained by the regression model across the 50 repetitions of the nested CV procedure for different adaptive filter configurations (N and λ). Using a linear regression model with the nine features from [6], the minimum average MAE was obtained with $N = 3$ harmonics and $\lambda = 0.9999$. In general, adding more harmonics did not further decrease MAE. This result is consistent with [6], where the RLS filter was used with $N = 4$.

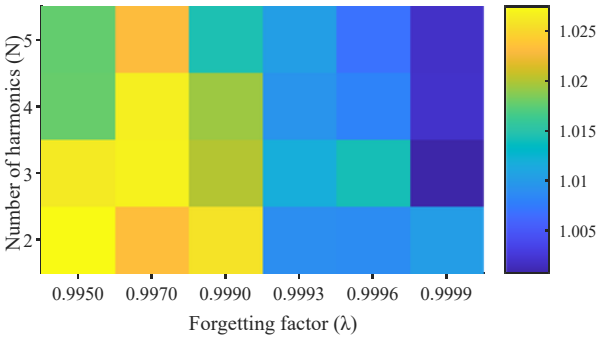

Figure 2. Average MAE over 50 repetitions of the nested CV, as a function of λ and N.

Figure 3 shows the average MAE as a function of the number of features (V) used in the SVR regression model over the 50 repetitions. This analysis was performed using the RReliefF feature selection algorithm mentioned above. The results were compared with two other algorithms: MRMR, a filter method that maximizes relevance and minimizes redundancy; and Plus-l take away-r (PTA), a wrapper method that combines sequential forward and backward selection to minimize the MAE. In this study, PTA(3,2) was used, adding the three most relevant variables and removing the two least informative ones at each iteration.

As can be observed, PTA(3,2) maintains a low and stable MAE even for models including a very small number of variables. In contrast, the filter methods (MRMR and RReliefF) show a progressive decrease in MAE as the number of features included in the model increases, reaching a minimum at 9 and 14 features for MRMR and RReliefF, respectively. Including additional features resulted in an increase in MAE. The CO estimation model with the lowest MAE (0.96 L/min) was based on 14 features selected using the RReliefF algorithm.

The selection probability of each feature, estimated as the proportion of times it was selected in a model with K

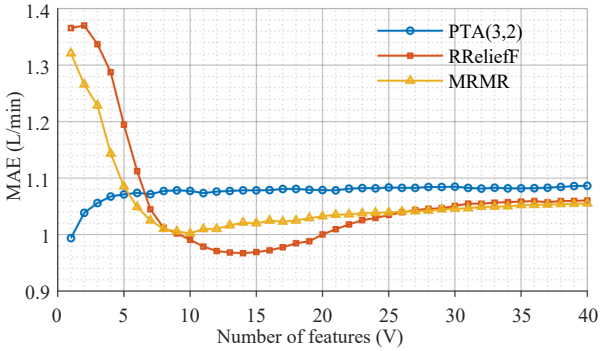

Figure 3. Average MAE of the CO estimation model over the 50 repetitions of the nested CV procedure when different feature selection algorithms are used.

features, is shown in the heatmap in Figure 4. The analysis reveals an initial predominance of $CC^c(n)$ features — skewness (skw^c), and the mean (PW^c) and standard deviation ($stdPW^c$) of the pulse width— followed by uncorrelated information from $CC^a(n)$ —the mean pulse width (PW^a), and the mean onset-to-peak (D_1^a) and peak-to-end (D_2^a) durations of the fluctuations—.

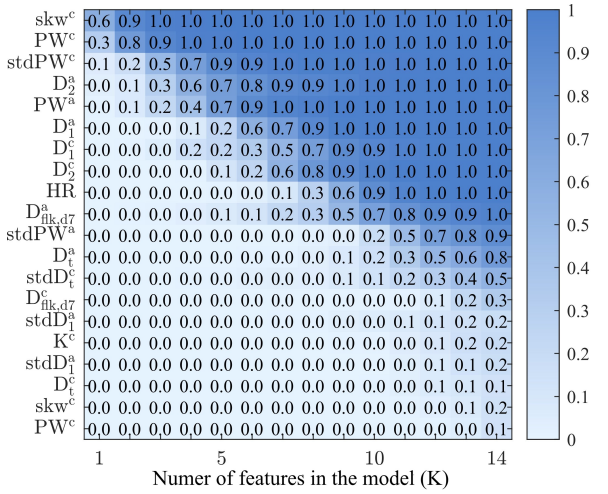

Figure 4. Inclusion probability of features in a model with K features.

5. Conclusions

This study presents a technical framework that combines advanced biomedical signal processing and machine learning techniques to non-invasively estimate CO. It uses ECG and BCG signals, isolates the circulatory components of both BCG signals through adaptive filtering and SWT-based multiresolution analysis, and feeds a SVR regression model with the most relevant features extracted from both circulatory components. The regression model showed MAE of 0.96 L/min, equivalent to a relative error of approximately 14 % (considering the mean CO of 6.7 L/min). Given the reduced sample size (20 subjects), these results should be interpreted as a proof of concept; validation on a larger and more heterogeneous cohort is required to confirm generalizability. We hypothesize that CO accuracy matters most in stable patients, while trend tracking may be equally relevant in unstable ones. Accuracy could be improved by incorporating impedance, capnography, and photoplethysmography signals already available in prehospital devices. The method remains easy to deploy and cost-effective, and could be integrated into prehospital defibrillation equipment. This framework lays the groundwork for continuous non-invasive circulation monitoring that could ultimately improve emergency medical care and increase survival rates in the most critical cases.

Acknowledgments

This work was partially funded by the Spanish Ministry of Science, Innovation and Universities through project PID2024-159268OB-I00, jointly with the European Regional Development Fund (ERDF); by the Basque Government through grants IT1853-26, 2023333017, 2024333037, and 2025333027; and by the University of the Basque Country (UPV/EHU) through project EHU-N25/75.

References

[1] Tsao CW, et al. Heart disease and stroke statistics–2022 update: a report from the american heart association. Circulation 2022;145(8):e153–e639.

[2] Sondergaard KB, et al. Bystander cardiopulmonary resuscitation and long-term outcomes in out-of-hospital cardiac arrest according to location of arrest. Eur Heart J 2019; 40(3):309–318.

[3] Jagarlamudi NS, et al. Unveiling breakthroughs in post-resuscitation supportive care for out-of-hospital cardiac arrest survivors: a narrative review. Cureus 2023;15(9).

[4] Tibballs J, Weeranatna C. The influence of time on the accuracy of healthcare personnel to diagnose paediatric cardiac arrest by pulse palpation. Resuscitation 2010;81(6):671–675.

[5] Alonso E, Irusta U, Aramendi E, Daya MR. A machine learning framework for pulse detection during out-of-hospital cardiac arrest. IEEE Access 2020;8:161031–161041.

[6] Svensøy JN, et al. Cardiac output estimation using ballistocardiography: a feasibility study in healthy subjects. Sci Rep 2024;14(1):1671.

Address for correspondence:

Sara Entenza
Plaza Ingeniero Torres Quevedo, 1, 48013 Bilbao
sara.entenza@ehu.eus